Exploiting Diurnal User Mobility for Predicting Cell Transitions

Nandish P. Kuruvatti, Andreas Klein, Jörg Schneider, Hans D. Schotten
Institute for Wireless Communications and Navigation
University of Kaiserslautern
Email: {kuruvatti,aklein,schneider,schotten}@eit.uni-kl.de

***Abstract*—Mobility of commuters is not purely random but rather direction oriented and may be learned after monitoring user movements for a couple of business days. Exploiting movement data and context information of diurnal user movements (public transportation, vehicular users, etc.) allows for predicting cell transitions and lays the basis e.g. for designing efficient resource reservation schemes or smart resource mapping approaches. In real life scenarios, several mobile users co-travel in public transport forming data intensive moving user clusters or moving networks [12]. Various load balancing solutions exist to manage congestion situations that could arise [4][5]. However, the crucial trigger for these solutions is timely prediction of arrival of moving user clusters or moving networks into a cell. This paper presents prediction and detection schemes that exploit context information for predicting user cell transitions and resulting congestion. These schemes are utilized to anticipate the arrival of data intensive moving user groups/moving networks, which are also referred to as "hotspots", into a cell. Simulation results demonstrate robust and timely prediction of these events and their applicability for handover optimization and smart resource management even at high velocities.**

***Index Terms*- Moving network, moving user cluster, hotspot, cell transition prediction, diurnal mobility, context information**

I. Introduction

The advancement in cellular technologies as well as user equipments (UEs) has led to a drastic growth of mobile subscribers. By the end of 2011 [2], the total number of mobile subscriptions was around 6 billion and is expected to reach approximately 9 billion by 2017. Forecasts of few telecom companies [1][2] indicate that wireless traffic growth will be in order of 1000 times larger in 2020 as opposed to 2010. Further, in day to day scenarios such as public transportation (e.g. buses, trains), where groups of mobile users are traveling together, the data traffic demanded by these users is massive due to growing popularity of mobile multimedia services [1]. In a vehicle with advanced communication and networking capabilities, a mobile router situated within vehicle could be managing all user connections in the vehicle, in turn limiting required UE transmit powers. This constellation is referred to as moving network and may become reality in the not too distant future as stated in [10]. In contrast, a group of users traveling in a conventional vehicle, where connections are individually managed by the serving base station (BS), is referred to as moving user cluster. These variants are expected to travel within service areas of mobile network providers, leading to dynamically changing and potentially high traffic demands. Given the forecasts, data traffic demands of moving networks/user clusters will keep increasing and will impose challenges on traffic and mobility management. One of the most significant problems caused by data intensive moving user clusters or moving networks is congestion due to "hotspot" situation in a cell. The hotspot caused by such moving entities can be classified as preferential mobility based hotspot [3]. Several conventional techniques such as mobility load balancing [4], channel borrowing [13], coverage adaptation, etc. [5][14] exist to combat hotspot. Further novel approaches for smart resource mapping in context aware multi-RAT scenarios are in their inception [6]. However, the basis for these solutions is prediction and detection of arrival of data intensive moving networks/user groups into a cell. There are several schemes in literature which investigate hotspot situation based on network load, blocking or dropping rates [3][7]. The majority of works considers high user arrival rate, low departure rate, or increased bandwidth demand of existing users leading to hotspot in a cell [3]. Although, these are good theoretical representation of hotspot, it is not beneficial to consider such a model in real world hotspot scenarios caused by moving user clusters or moving networks. The work presented in this paper emphasizes on hotspot problem resulting from moving networks/user groups. An approach based on movement estimation is presented to predict and detect arrival of moving networks/user groups into a cell. User cell transitions are predicted well in advance and this context is beneficially applied for pro-actively triggering load balancing mechanisms as potential countermeasures for combating congestion.

Outline. Section II deals with methods to predict cell transitions of moving users, section III discusses simulation scenarios and results, and section IV provides conclusion and indicates future work.

II. Cell Transition Prediction

Almost all types of public transportation, such as trains, buses, and trams, follow diurnal mobility [8]. Mobility of commuters is not purely random but rather direction oriented characterized by origin and destination points [8]. When such mobility is confined to urban regions, the probability of hotspot occurrence is high in cells through which it traverses. Whenever a mobile hotspot is detected in a cell, it is beneficial to predict the next cell to which this moving user group/moving network would travel. This enables prediction of hotspot situation in near future of neighboring cells.

A. Diurnal Mobility Model

In case of random walk mobility model a user can travel in all six directions with equal probability from its current cell. However in diurnal mobility model (as depicted in Fig. 1),

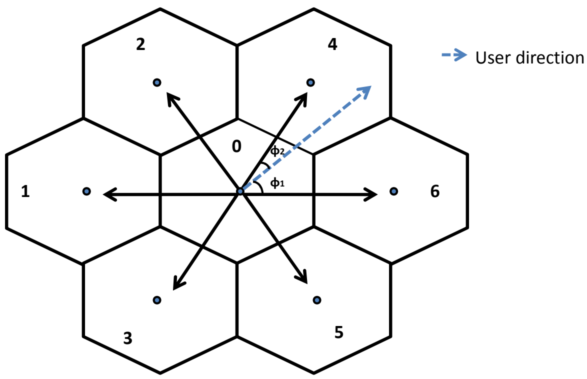

Fig. 1. Diurnal mobility model

user group direction is probable in only two directions (e.g. streets, train tracks) and zero in other directions [8]. Hence, a user group can transit into one of the two adjacent cells from its present cell. If ϕ_1 and ϕ_2 are the angles of users' direction with respect to the closest directions leading towards center of neighboring cells, then probability of user transition into those neighbors are [8],

$$p_1 = \left(1 - \frac{\phi_1}{60}\right) \tag{1}$$

$$p_2 = \left(1 - \frac{\phi_2}{60}\right) \tag{2}$$

B. Estimation of User Direction

In this section the different approaches for sampling user positions and for estimating user directions are described. The model employs a "virtual" circle inscribed in each cell. This "virtual" circle corresponds to a certain signal strength threshold derived from radio propagation data. The center of circle coincides with center of cell. The position of user is estimated at fix, but velocity-dependent intervals. The user positions falling in the circle are recorded and used to estimate direction. The user angle is calculated at each position as,

$$\phi = \tan^{-1}\left(\frac{y_2 - y_1}{x_2 - x_1}\right) \tag{3}$$

where (x_2,y_2) and (x_1,y_1) are present and previous positions, respectively.

Different methods for estimating user direction are depicted in Fig. 2. Method 0 utilizes average of all user angles recorded in the circle to estimate user direction, whereas method 1 only considers average of user angles recorded within the circular strip. Method 2 performs exponential moving average (EMA) [11] on the user angles recorded in the circle and method 3 uses only instantaneous angle of user before leaving the "virtual" circle. In certain special cases users will not enter the circular region, as depicted in Fig. 3. In order to estimate user direction in such cases, the following algorithm is employed:

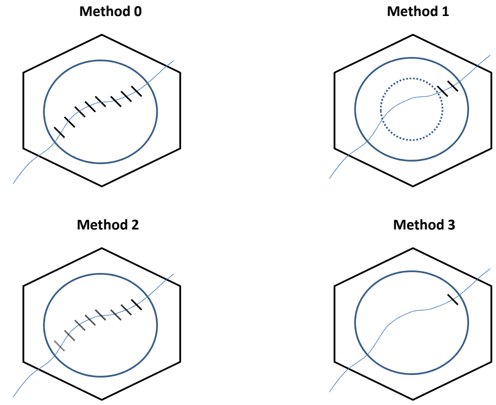

Fig. 2. Direction estimation methods

1) The distance of user from cell center is monitored at fixed logging intervals.
2) IF the distance is greater than radius of circle: GOTO step 3, ELSE: user is in the circle, STOP.
3) IF present distance is greater than previous distance: user will not enter the circle, ELSE: repeat step 2.
4) Instantaneous user angle is used to estimate direction.

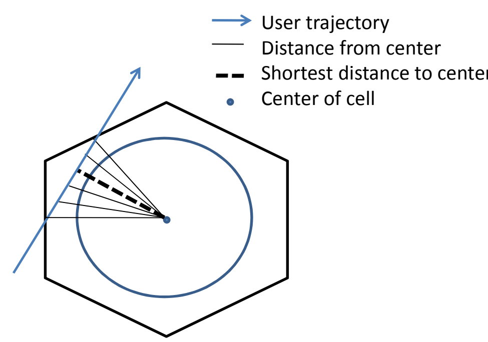

Fig. 3. User not entering recording circle

C. Prediction of Cell Transition Based on Angular Deviation

The user abiding to diurnal mobility can transit from its present cell to one of the two neighboring cells [8] influenced by its direction. Table. I lists potential next cells for such user in cell 0, as shown in Fig. 1, based on user angle. Similarly, next cells can be stated for each cell in the cellular layout. The probability of transition to next cells is given by Eq. 1 and Eq. 2.

TABLE I. Next cell based on user angle

User angle ϕ	Set of Next Cells	ϕ_1	ϕ_2
0-60	6,4	ϕ	$60-\phi$
60-120	4,2	$\phi-60$	$120-\phi$
120-180	2,1	$\phi-120$	$180-\phi$
180-240	1,3	$\phi-180$	$240-\phi$
240-300	3,5	$\phi-240$	$300-\phi$
300-360	5,6	$\phi-300$	$360-\phi$

D. Comparison of Direction Estimation Methods

At high velocity and straight motion of users, all methods mentioned in Fig. 2 yield same prediction results. When user trajectory deviates within angular range for same next cells (e.g. $0-60°$), all approaches predict same set of next cells, although estimated directions are different. This is illustrated by trajectory A in Fig. 4 and the results at two different velocities (20 and 100 km/h) are listed in Table II. The actual next cell is 6.

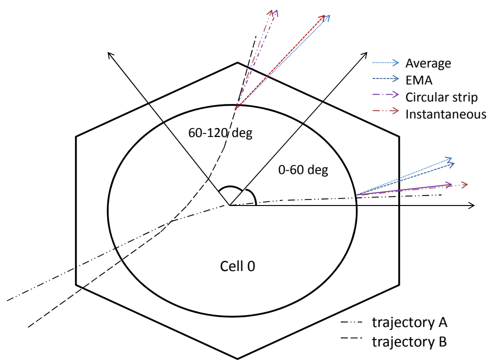

Fig. 4. Illustration of predicted directions for various user trajectories

In case the user trajectory deviates outside angular range for same next cells, instantaneous and circular strip-based approaches lead to prediction of actual next cells. EMA and average lead to prediction of different set of next cells, due to consideration of history values of angles. Such a scenario is depicted by trajectory B in Fig. 4 and the results at two different velocities (20 and 100 km/h) are listed in Table III, actual next cell being cell 4. For high velocities, sampling rate is to be adapted in order to yield robust estimation in particular for history-based approaches.

TABLE II. COMPARISON OF ESTIMATION METHODS (WITHIN RANGE)

Estimation Method	Velocity (km/h)	Angular Deviation	Set of Next Cells	P_1	P_2
Average	20	24.12	6,4	0.598	0.402
EMA		23.39	6,4	0.611	0.389
Circular Strip		18	6,4	0.7	0.3
Instantaneous		18	6,4	0.7	0.3
Average	100	24.6	6,4	0.59	0.41
EMA		21.4	6,4	0.643	0.357
Circular Strip		18	6,4	0.7	0.3
Instantaneous		18	6,4	0.7	0.3

TABLE III. COMPARISON OF ESTIMATION METHODS (OUTSIDE RANGE)

Estimation Method	Velocity (km/h)	Angular Deviation	Set of Next Cells	P_1	P_2
Average	20	55	6,4	0.084	0.916
EMA		56	6,4	0.067	0.933
Circular Strip		63	4,2	0.95	0.05
Instantaneous		65	4,2	0.917	0.083
Average	100	55	6,4	0.084	0.916
EMA		59	6,4	0.017	0.983
Circular Strip		65	4,2	0.917	0.083
Instantaneous		65	4,2	0.917	0.083

E. Prediction of Cell Transition Based on Distance

The user movements indicated in green and blue lines in Fig. 5 have the same estimated user direction (angle). But the next cell of transition depends on position of user trajectory at the circumference of the circle. At the point of prediction,

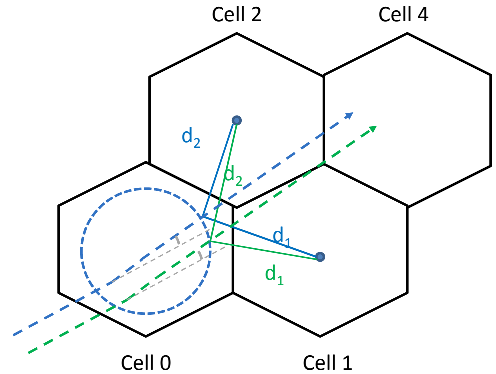

Fig. 5. Cell transition prediction based on distance

if d_1 and d_2 are the distances of user from centers of cell 1 and cell 2 then probabilities of transition to these cells based on distance are,

$$p_1 = 1 - \frac{d_1}{d_1 + d_2}, \tag{4}$$

$$p_2 = 1 - \frac{d_2}{d_1 + d_2}, \tag{5}$$

F. Combined approach

Probabilities of transition are different for angle-based and distance-based methods. The probabilities can be combined by taking average of the two. However, distance based approach is observed to have more impact on probability than method employing user angle. Hence, the distance component of probability equation is weighed by $\alpha > 1$. The probability equations of the combined approach are,

$$p_1 = 1 - \frac{\phi_1}{60(1+\alpha)} - \frac{\alpha}{1+\alpha} \cdot \frac{d_1}{d_1 + d_2}, \tag{6}$$

$$p_2 = 1 - \frac{\phi_2}{60(1+\alpha)} - \frac{\alpha}{1+\alpha} \cdot \frac{d_2}{d_1 + d_2}, \tag{7}$$

G. Special Case

In Fig. 6, user is traveling from cell 3 following diurnal mobility. In normal case user always transits to one of the two next cells based on its direction [8]. In special case, a brief transition (indicated in red) happens to a third cell before moving to probable next cell. For instance, in cell 6 it is estimated that cell 15 and cell 18 are the next cells when relying on angle-based method. But user briefly travels to cell 4 which cannot be traced.

The brief transition to a third cell could be predicted by considering three potential next cells instead of two for each user direction range. The probabilities of transition in these cells based on angle [8] are,

$$p_1 = \left(1 - \frac{\phi_1}{60}\right) \tag{8}$$

$$p_2 = \left(1 - \frac{\phi_2}{60}\right) \tag{9}$$

$$p_3 = 0 \tag{10}$$

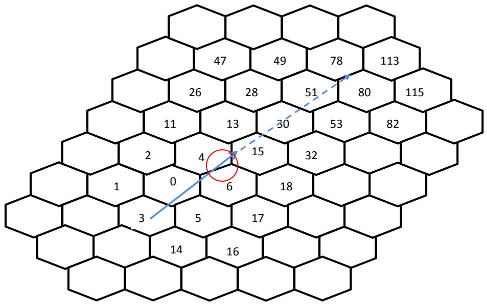

Fig. 6. User trajectory in special case

At prediction point, if d_1, d_2, and d_3 are distances of user from centers of next cells then probabilities based on distance are,

$$p_1 = 1 - \frac{d_1}{d_1 + d_2 + d_3}, \quad (11)$$

$$p_2 = 1 - \frac{d_2}{d_1 + d_2 + d_3}, \quad (12)$$

$$p_3 = 1 - \frac{d_3}{d_1 + d_2 + d_3}, \quad (13)$$

Combined probabilities similar to section II-F are given by,

$$p_1 = \frac{3+2\alpha}{3(1+\alpha)} - \frac{\phi_1}{60(1+\alpha)} - \frac{\alpha}{1+\alpha} \cdot \frac{d_1}{d_1+d_2+d_3}, \quad (14)$$

$$p_2 = \frac{3+2\alpha}{3(1+\alpha)} - \frac{\phi_2}{60(1+\alpha)} - \frac{\alpha}{1+\alpha} \cdot \frac{d_2}{d_1+d_2+d_3}, \quad (15)$$

$$p_3 = \frac{2\alpha}{3(1+\alpha)} - \frac{\alpha}{1+\alpha} \cdot \frac{d_3}{d_1+d_2+d_3}, \quad (16)$$

III. Simulation Results

A system-level simulator is used and a multi-cell scenario is created as illustrated in Fig. 6 with a BS at each cell center. The considered radio access technology is LTE. The cluster of 60 users moving together at high velocity (120 km/h) constitutes a mobile hotspot. Each cell is allowed to have static background users. Evaluation methodology follows [9] and assumes 10 MHz bandwidth for LTE operation at 2 GHz. The trajectory followed by moving user group is as in Fig. 6. Table IV summarizes simulation parameters.

TABLE IV. Simulation Parameters

Parameter	Assumption
Carrier frequency	2 GHz
System bandwidth	10 MHz (50 PRBs)
Total transmit power	40 W/250 mW ($s2s = 500$m/200m)
Control channel overhead	12%
Shadowing	log-normal Standard deviation: 8 dB Decorrelation distance: 50 m
Fast fading	2-tap Rayleigh fading channel
Noise power	-174 dBm/Hz + $10 \cdot \log_{10}(B) + 7$
Background users per cell	30
Hotspot users	60 at 120 km/h

Table V shows results of next cell prediction for user trajectory in Fig. 6 from cell 3 to cell 15.

TABLE V. Next Cell Prediction Results

Present Cell	Next Cells	P_{angle}	$P_{distance}$	$P_{combined}$
Cell 3	Cell 5	0.25	0.346	0.327
	Cell 0	0.75	0.410	0.478
	Cell 1	0	0.243	0.194
Cell 0	Cell 6	0.25	0.447	0.408
	Cell 4	0.75	0.353	0.433
	Cell 2	0	0.198	0.158
Cell 6	Cell 18	0.25	0.202	0.211
	Cell 15	0.75	0.332	0.416
	Cell 4	0	0.465	0.372
Cell 4	Cell 15	0.25	0.468	0.424
	Cell 13	0.75	0.311	0.399
	Cell 11	0	0.219	0.175

From the table, it could be observed that the angle-based approach can't trace transition into a third cell and its probability is always zero. This limitation is also reflected in combined approach, affecting prediction accuracy even with high values of α. The affect of α on prediction of next cell during brief transition (special case) is described in Fig. 7. With increase in value of α, prediction in actual next cell by combined approach improves but does not exceed the probability of prediction in other cell (e.g. next cell 2 in Fig. 7). Fig. 8 illustrates the comparison among distance based, angle based and combined approaches in predicting transition into actual cell. It could be seen that distance based approach makes best prediction with consistency among the three.

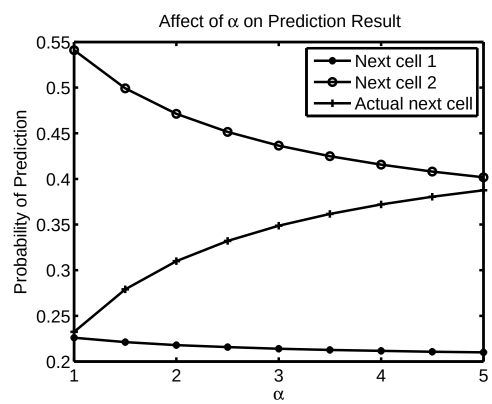

Fig. 7. Affect of α on Prediction Probability

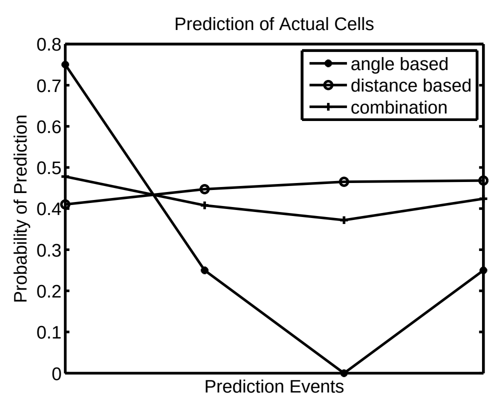

Fig. 8. Comparison of Prediction Approaches

The earliness of next cell prediction could be improved by reducing radius of recording circle. However this has a tradeoff with accuracy of prediction. Further, prediction at low velocity is earlier than at high velocity since there is a longer period of time (dwelling period) between prediction and actual transition at lower velocities.In general, prediction of hotspot and next cell transition are easier at low velocities and becomes challenging at high velocities. The simulations are carried out for site-to-site distances ($s2s$) of 500m and 200m (dense deployment), respectively. The moving user group travels same distance in both cases. Load balancing (LB) mechanism is triggered in respective cells which anticipate arrival of moving networks/user groups enabled by prediction of user cell transitions. This procedure relieves congestion and accommodates for approaching moving networks/user groups. This is reflected by reduced dropping of connections, reduction in blocked access attempts, and decrease in blocked handovers at respective BSs. There is only a very slight decrease (1%) in load, since the freed up resources will soon be occupied by moving networks/user groups. The average reduction in these KPIs using LB triggered by cell transition prediction for $s2s = 500$m and $s2s = 200$m, respectively, are illustrated in Fig. 9 and Fig. 10. These results demonstrate that prediction

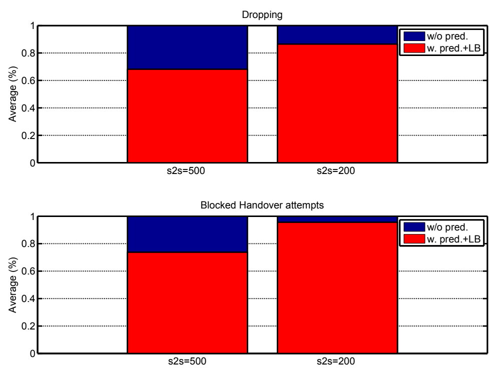

Fig. 9. Dropping and blocked HO attempts

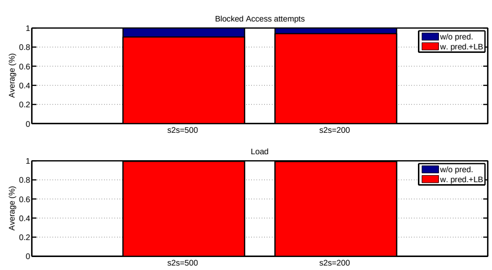

Fig. 10. Blocked access attempts and load

of user cell transitions could be exploited to anticipate arrival of moving networks/user groups into a cell and, thus laying a basis for context-aware radio resource management. The results show the validity of these schemes even at high velocities as well as dense deployments, which are envisioned to spread in future [1][10].

IV. Conclusion and Future Work

The primary step to mitigate congestion issues caused by moving user groups/networks is to predict their arrival into a cell. This paper presented and evaluated methods for hotspot prediction with an emphasis on moving user clusters/networks. The diurnal mobility of users, that can be learned after monitoring user movements for a couple of business days, is exploited to predict cell transitions. This context information is utilized to trigger load balancing as a potential countermeasure to combat eminent congestion. Simulation results demonstrate the ability of presented approaches to predict arrival of moving user groups/networks well in advance, maintaining consistency even at high velocities. Future work aims at applying these prediction approaches for designing smart radio resource management and load balancing strategies in heterogeneous and ultra-dense deployments.

V. Acknowledgment

Part of this work has been performed in the framework of FP7 project ICT-317669 METIS, which is partly funded by the European Union. The authors alone are responsible for the content of the paper.

References

[1] Nokia Siemens Networks, *2020: Beyond 4G Radio Evolution for the Gigabit Experience*, white paper, Aug., 2011.

[2] Ericsson, *More than 50 billion connected devices*, white paper, Feb., 2011.

[3] J. Jobin, M. Faloutsos, S. K. Tripathi and S.V. Krishnamurthy, *Understanding the Effects of Hotspots in Wireless Cellular Networks*, INFOCOM 2004.

[4] A. Lobinger, S. Stefanski, T. Jansen, and I. Balan, *Load Balancing in Downlink LTE Self-Optimizing Networks*, 71st IEEE Vehicular Technology Conference (VTC-Spring), May, 2010.

[5] A. Sharma, A. Roy, S. Ghosal, R. Chaki and U. Bhattacharya, *Load balancing in Cellular Network: A review*, International Conference on Computing, Communication & Networking Technologies (ICCNT) 2012.

[6] A. Klein, C. Mannweiler, J. Schneider, F. Thillen and H.D. Schotten, *A concept for context-enhanced heterogeneous access management*, IEEE Globecom workshops 2010.

[7] Y.K Tang, J. Misic, H. Zhu and I. Chlamtac, *An Online Hotspot Detection Scheme in DS-CDMA Networks - Single Traffic Type*, IEEE Globecom 2004.

[8] S.K. Sadhukhan, S. Mandal, P. Bhaumik and D. Saha, *A Novel Direction-Based Diurnal Mobility Model for Handoff Estimation in Cellular Networks*, IEEE India conference (INDICON) 2010.

[9] 3GPP TSG RAN, *Further advancements for E-UTRA physical layer aspects (Release 9)*, TR 36.814 V9.0.0, March, 2010.

[10] METIS, *D1.1 - Future radio access scenarios, requirements and KPIs*, May, 2013, available online: https://www.metis2020.com.

[11] D. Haynes, J. Misic, S. Corns and G.K Venayagamoorthy, *An Exponential Moving Average algorithm*, IEEE Congress on Evolutionary Computation 2012.

[12] J.I Agbinya, *Design concepts: wireless moving networks (WMN)*, The 6th International Conference on Advanced Communication Technology, 2004.

[13] Quan Lin, L. Nahar and S. Bhattacharya, *A remote channel borrowing approach for real-time congestion control in wireless communication*, IEEE Globecom 1997.

[14] C. Askarian and H. Beigy *A Survey for Load Balancing in Mobile WiMAX Networks*, Advanced Computing: An International Journal (ACIJ), Vol.3, No.2, March 2012.